

# The Kyoto road piled embankment: 3<sup>1</sup>/<sub>2</sub> years of measurements

Van Eekelen, S.J.M. and Bezuijen, A.  
Deltares and Delft University of Technology

Alexiew, D.  
HUESKER Synthetic GmbH

Keywords: Piled embankment, geogrids, arching, full-scale test, field monitoring

## ABSTRACT:

Field measurements on a flat reinforced piled embankment (the Kyoto Road) are reported and evaluated. It was constructed on 13 m long timber piles with 1.27x1.27 m<sup>2</sup> spacing with concrete pile caps of 0.3 m diameter and reinforced by two layers of high-modulus low-creep uniaxial geogrids. On top of that, a 1.15 m high embankment was constructed. A monitoring program was carried out for more than three years. The measurements included the forces on the pile caps, on the geogrid, (indirectly) the upward reaction of the soft subsoil between the caps underneath the geogrid and the pore water pressures. The measurements show among others the development of arching over time, the disturbing effects of heavy dynamic traffic followed by arching recovery etc. The measurements are compared with predictions of several codes, such as the German EBGEO, the British Standard BS8006, but also with a modified BS8006. The EBGEO is in best agreement with the measurements.

## 1 INTRODUCTION

In 2009, the Dutch Design Guideline for the increasingly popular reinforced piled embankments has been presented. To come to this Guideline, major parts of the German EBGEO have been adopted (Eekelen et al, 2010) and adapted to typical Dutch aspects, such as relative low embankment height and to the Dutch safety procedures.

For this Guideline, existing design procedures for reinforced embankments on piles were considered and compared with measurements from several piled embankments. This paper considers one of these monitored piled embankments: the Kyoto Road. Measurements are compared with predictions. The first two years of the measurements results have been reported earlier (Eekelen et al. 2008b).

This paper presents 3<sup>1</sup>/<sub>2</sub> years of measurements and focuses on the measured pore pressures, the influence of the dynamic traffic load, and the influence of the tensile stiffness of geosynthetic reinforcement (GR) and modulus of subgrade reaction on the calculations. The calculation of the tensile force in the GR due to the vertical loads and the arching is considered. The (often-significant) tensile forces due to the horizontal stresses in the embankment (“spreading”) are of no importance due to the flat geometry of the Kyoto Road and beyond the scope of this study.

## 2 LOAD DISTRIBUTION

To compare the calculated and measured load distribution, load parts *A*, *B* and *C* are defined as (Fig. 1):

- Load part *A* is transferred directly to the pile caps through arching,
- Load part *B* is transferred through the reinforcement to the pile caps,
- Load part *C* is resting on the soft subsoil

In this paper *A*, *B* and *C* are given in kN.

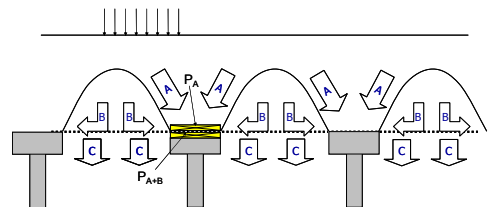


Figure 1. Load distribution in a piled reinforced embankment. Definitions of *A*, *B* and *C*. The total pressure cells  $P_A$  and  $P_{A+B}$  measure respectively *A* and (*A*+*B*).

### 3 THE KYOTO ROAD

#### 3.1 Layout of the system

The 'Kyoto Road' in Giensburg in the Netherlands is shown in Figure 2.

The system consisted of 13 m long timber piles with a 1.27x1.27 m<sup>2</sup> CC-spacing, concrete pile caps (diameter of 0.3 m), geogrid reinforcement and 1.15 m of compacted fill (silty sand mixture).

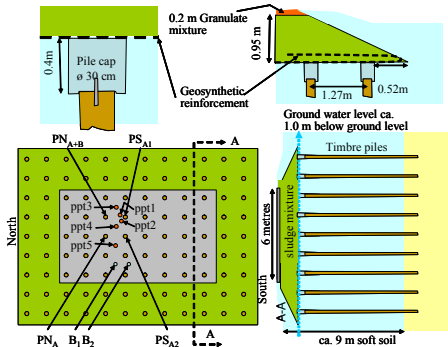


Figure 2. Layout of the Kyoto Road

Two geogrid layers were installed: Fortrac<sup>R</sup> 350/30-30 M along the road axis (bottom) and Fortrac<sup>R</sup> 400/30-30 M across. Figure 3 shows their isochrones: the time-dependent tensile stiffness *J* can be evaluated (Table 1, for a strain of 2%).

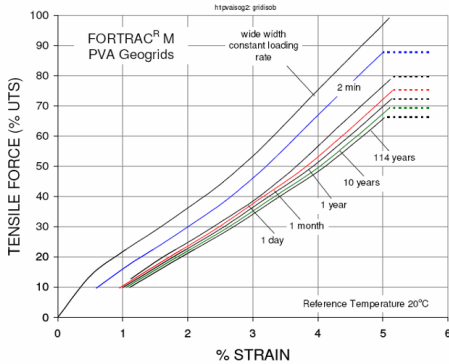


Figure 3. Isochrones of the geogrids used.

Along road axis/ perpendicular to road axis	Time under load	Ultimate tensile strength UTS (kN/m)	Tensile stiffness <i>J</i> (kN/m) <i>J</i> = (% of UTS / strain) x UTS Herein values at 2% strain
along	1 day	350	(25,0/2)*350 = 4375
perpendicular	1 day	400	(25,0/2)*400 = 5000
along	1 year	350	(22,8/2)*350 = 3990
perpendicular	1 year	400	(22,8/2)*400 = 4560
along	10 years	350	(22,1/2)*350 = 3868
perpendicular	10 years	400	(22,1/2)*400 = 4420

Table 1. Tensile stiffness of geogrid reinforcement

#### 3.2 Subsoil

The local soil was excavated to 1.15 m to remove rubbish. Immediately after that, the Kyoto Road was constructed in less than four days. Thus, the subsoil did not have the chance to swell before the piles and embankment were installed. Table 2 gives the Young's moduli *E* as determined from the compression tests carried out before construction.

		Thickness (m)	<i>E</i> (kN/m <sup>2</sup> )
Top layer	peat	<i>d</i> <sub>1</sub> = 1,45 m	1077
Second layer	clay	<i>d</i> <sub>2</sub> = 1,50 m	2000

Table 2. Young's moduli of subsoil

From this, the modulus of subgrade reaction *k* can be calculated:  $k = (E_1 * E_2) / (E_1 * d_2 + E_2 * d_1) = (1077 * 2000) / (1077 * 1,5 + 2000 * 1,45) = 477 \text{ kN/m}^3$ .

This is probably a lower value than in practice 'felt' by the embankment, because the subsoil did not swell between excavation and construction. Furthermore, at the end of the construction the ground pressures will be lower than they have been before, so that the behaviour should be stiffer.

#### 3.3 Properties of fill

The fill is a dredged silty sand with some additives containing mainly clay and cement. It was used herein because of the environmental-friendly re-use of waste material. Usually, non-cohesive granular material is used for embankment fills. Table 3 shows the properties of the fill.

$\gamma_{wet}$	$\gamma_{dry}$	$\gamma_{average}$	<i>W</i>	<i>K<sub>v</sub></i>	$\phi$	<i>c</i>
kN/m <sup>3</sup>	kN/m <sup>3</sup>	kN/m <sup>3</sup>	%	m/s	°	kPa
22.2	17.0	18.6	18.1	2.1 E-9	33.8	11.5

Table 3. Properties of fill. ( $\gamma$  unit weight, *W* water content, *K<sub>v</sub>* the vertical permeability,  $\phi$  internal friction angle and *c* cohesion.

#### 3.4 Monitoring in the Kyoto Road

Monitoring from November 2005 to May 2009 included the total forces just on top of piles, both on top of the reinforcement (PS<sub>A</sub> and PN<sub>A</sub> in Figure 2) as well as below the reinforcement (PN<sub>A+B</sub>), the ground water level and the pore pressures below the embankment (locations of the piezometers (ppt) in Figure 2, depths: in Figure 5).

#### 3.5 Measurement results

Figures 4 and 5 show the measured pile forces and pore pressures. Ppt 1 and 2 are installed relatively close to a pile and relatively deep. They measure mainly the excessive pore pressures due to pile installation. The other 3 ppt's give the influence of the load of the embankment on the non-swollen subsoil. During a period of a few months, they reduce due to consolidation. An excessive pore pressure of ca. 10 kPa remains. As expected, the subsoil support C re-

duces during the consolidation, however, later C increases again a bit (Fig. 4 & 5).

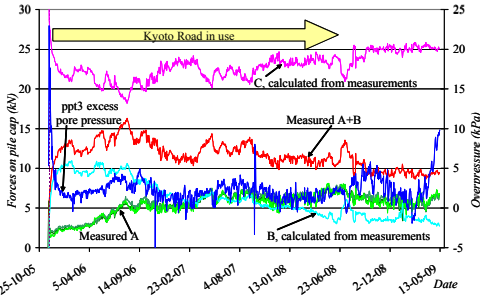


Figure 4. Measured pile forces and excess water pressures

Traffic started immediately after construction. Arching needed some months to develop completely (increasing A, decreasing B, C and pore pressures). Other monitoring projects (Haring et al, 2008 & Van Duijnen et al, 2010) also show that arching could improve with time under operation.

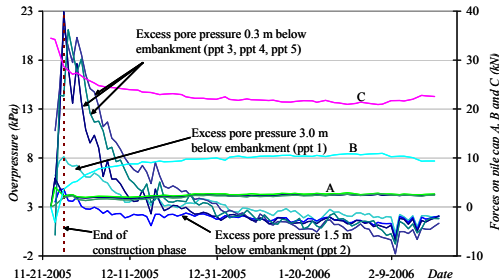


Figure 5. Measured excess pore pressures and pile forces

This improvement could be caused by the increase of the internal friction angle due to densification, some hydraulic binding, some increase of GR deflection due to creep and subsoil settlement, shown by the measured reduction of the pore pressures during the first months.

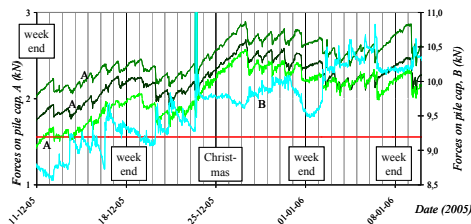


Figure 6. Daily arching cycle in the Kyoto Road

A heavy dynamic load, however, can cause a sudden short-term decrease of arching (A decreases and B increases suddenly). The Kyoto Road experiences both sudden reductions in arching and an on-

going development of the arching during several months (increasing A) or years (decreasing B). The system only experiences traffic during working hours, and then usually mainly heavy trucks. Figure 6 shows a daily arching reduction during the first passages of the day. Figure 7 shows the increase of B after a passage of a rather heavy truck. After that, the arching generally recovers during the rest of the day or weekend, although other passages occur.

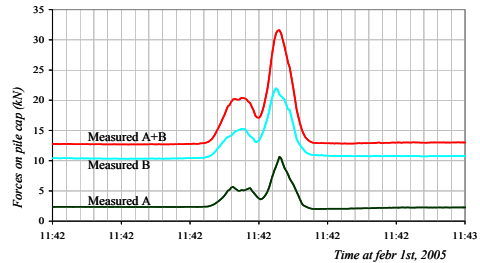


Figure 7. Passage of a truck, 397 kN, divided over 2\*2 axles. Measurements of  $PN_A$  and  $PN_{A+B}$

From July 2006 on B (and thus the tensile force in the geosynthetic) continuously reduces slightly (Fig. 4 & 5) and A continuously increases. The variations are mainly caused by climatic circumstances. (A+B) still decreases slightly, which implies that C increases (see also Fig. 8).

### 3.6 Predictions

Figure 8 compares the measurements with two EB-GEO and two BS8006 predictions. The tensile forces were not measured; the predictions are compared in Table 4. The four predictions are:

1. EBGEO with subsoil support, several moduli of subsoil reaction  $k$ .
2. EBGEO without subsoil support ( $k=0$ )
3. Modified BS8006 as described by Van Eekelen & Bezuijen, 2008.
4. Original BS8006, Jones et al. (1990). In the 2009-draft version of BS8006 the considered equations have not been changed.

For all BS8006 calculations the input strain (has to be assumed) has been adapted to correspond to the tensile moduli of the geogrids  $J = 4375/3990/3868$  kN/m (Table 1) for 1 day/1 year/10 years.

### 3.7 Comparison of measurements and predictions

The differences between predictions for short- and long-term tensile stiffness of the geogrids are minimal due to their low creep (Fig. 3 & Table 1). However, the long-term measurements show a constantly slightly increasing C indicating that some creep (GR deflection) takes place as expected.

The differences in the predictions for different  $k$  ( $k = 0$ ,  $k = 477$  and  $k = 1000$  kN/m<sup>3</sup>) are considerable. A good agreement of predictions vs. measure-

ments is found for EBGEO with  $k = 1000 \text{ kN/m}^3$ . Apparently, in this case the subsoil has in fact a higher  $k$  than the determined one of  $477 \text{ kN/m}^3$ .

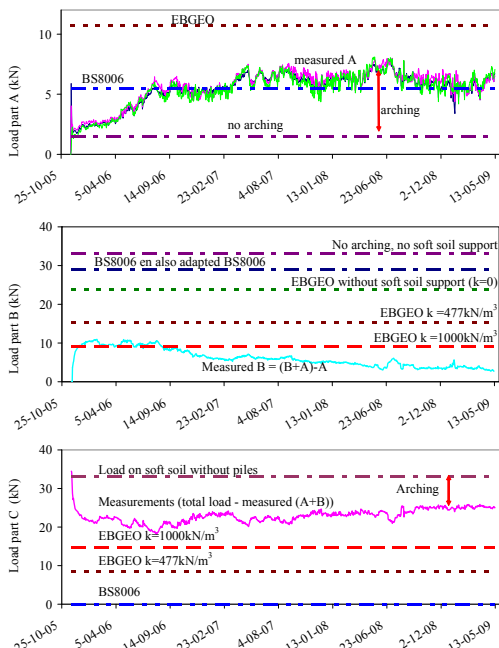


Figure 8. Comparison measured and predicted  $A$ ,  $B$  and  $C$ .

As discussed before,  $k$  as determined from compression tests is probably too low. Measurements in road N210 (Van Eekelen et al, 2010) also show as a tendency a larger contribution of the subsoil than EBGEO predicts with the  $k$  assumed for N210.

$k$ (kN/m <sup>3</sup> ) and $J$ (kN/m)	EBGEO with sub soil	EBGEO without sub soil	Modified BS8006	Original BS8006
$k = 477, J=4375$	55	85	85	120
$k = 477, J=3990$	53	82	82	117
$k = 477, J=3868$	52	81	81	116
$k = 1000, J=3990$	31	82	82	117

Table 4. Predictions of tensile force (kN/m) in geosynthetic reinforcement, depending on modulus of subgrade reaction ( $k$ , kN/m<sup>3</sup>), and the tensile stiffness of the GR ( $J$ , kN/m). Predictions of  $A$ ,  $B$  and  $C$  are shown in Figure 8.

Of course, design should be carried out with safety margins: the subsoil support can decrease due settlements, e. g. by more than 30% due to groundwater variations (Fig. 8 & Van Eekelen et al, 2008b).

Table 4 shows that for this geometry, the EBGEO without subsoil predicts the same tensile force as Modified BS8006.

## 4 CONCLUSIONS

The measurements in the Kyoto Road show that the arching develops over several months for the fill used, also under operation, and can vary. Heavy passages can provoke a temporary reduction of the arching.

The subsoil supports the embankment considerably, but with significant variations. The subsoil support is in the average still slightly increasing.

Measurements and predictions of EBGEO agree very well, especially when in the predictions a stiffer subsoil reaction than evaluated in the lab is chosen, which is probably a good, but difficult and sensitive choice.

The EBGEO without subsoil and Modified BS8006 give the same prediction for the tensile force in geogrids for this geometry.

## ACKNOWLEDGEMENTS

HUESKER Synthetic, Van Biezen Heipalen, Kantakun, Delft Cluster and Deltares for their contributions to the pilot project 'The Kyoto Road'.

## REFERENCES

- British Standard, BS8006, 1995. Code of practice for Strengthened/reinforced soils and other fills. (considered equations in 2009 draft version are the same).
- Duijnen, Piet van, Eekelen, Suzanne van, Stoel, Almer van der (2010). Holland's first railway on a LTP: Design against monitoring, to be published in the proc. of 9ICG, Brazil, 2010.
- EBGEO (2009), "Bewehrte Erdkörper auf punkt- oder linienförmigen Traggliedern", chapter 9: "Berechnung und Dimensionierung von Erdkörpern mit Bewehrungen aus Geokunststoffen". Deutsche Gesellschaft für Geotechnik e.V. (DGGT). Fachsektion "Kunststoffe in der Geotechnik" Arbeitskreis AK 5.2.
- Eekelen, S.J.M. van, Bezuijen, A. (2008a). Design of piled embankments, considering the basic starting points of the British Standard. Proceedings of EuroGeo4, Edinburgh, Sept. 2008.
- Eekelen, S.J.M. van, Bezuijen, A. Alexiew, Dimiter (2008b). Piled Embankments in the Netherlands: a full-scale test, comparing 2 years of measurements with design calculations. Proceedings of EuroGeo4, Edinburgh, Sept. 2008.
- Eekelen, Suzanne van, Jansen, Hein Duijnen, Piet van, Kant, Martin de, Dalen, Jan van, Brugman, Marijn, Stoel, Almer van der, Peters, Marco (2010). The Dutch Design Guideline for Piled Embankments, to be published in the proc. of 9ICG, Brazil, 2010.
- Haring, W., Profitlich, M. & Hangen, H.(2008). Reconstruction of the national road N210 Bergambacht to Krimpen a.d. IJssel, NL: design approach, construction experiences and measurement results. Proceedings of EuroGeo4, Edinburgh, Sept. 2008.
- Jones, C.J.F.P., Lawson, C.R., Ayres, D.J. (1990). Geotextile reinforced piled embankments. Geotextiles, Geomembranes and Related Products, Den Hoedt (ed.) 1990 Balkema, Rotterdam, ISBN 90 6191 119 2, pp 155-160